CLAS-Analysis 2013-102

Direct photoproduction of narrow baryon resonance in the reaction $\gamma p \to pK^0\bar{K}^0$ in CLAS

M. Amaryan, C. Nepali and G. Gavalian

Old Dominion University, Norfolk, VA

June 17, 2013

Contents

1 Introduction

In 2004, during g11a run period the CLAS Collaboration performed high statistics photoproduction experiment on hydrogen target to search for the Θ^+ pentaquark. As a result of the analysis of g11a data no signal of the Θ^+ pentaquark decaying to either pK^0 or nK^+ final state has been observed and an upper limit of Θ^+ photo-production cross section was reported in [1].

Recently we submitted a paper reporting observation of a narrow resonance structure at the mass $M(pK_L) = 1.543$ GeV via interference with ϕ meson production [2] from the same g11a data.

In this paper we present reanalysis of g11a data in a direct photo-production, without invoking interference with a ϕ meson production, following strategy of previous analysis [1]. However the difference of this analysis compared to the previous one [1] is first of all due to the reconstruction of the final state in the reaction $\gamma + p \to pK^0\bar{K}^0$ and secondly due to the Dalitz plot analysis of the three-body final state, which led to the observation of a narrow resonance structure in both the invariant mass of pK_S and pK_L at $M \sim 1.55$ GeV.

2 Experiment

The present study is based on the same data set collected in 2004 (g11a run period) using the CLAS [3] detector at TJNAF and analyzed previously in [1] and [2]. The experiment was performed using tagged photon beam produced through bremsstrahlung from a 4.02 GeV initial electron beam from the Continuous Electron Beam Accelerator Facility (CEBAF) at Jefferson Lab.

In this experiment the photon beam was incident on a 40 cm long liquid hydrogen target, centered 10 cm upstream from the center of the CLAS detector consisting of six equal sectors, equipped with time-of-flight scintillator counters, Electromagnetic Calorimeters, Drift Chambers and Čerenkov Counters, covering nearly 4π solid angle.

The CLAS standard particle identification scheme is used to select charged particles in the final state. The photon beam energy correction and charged particle momentum correction are based on the code developed by the g11 run group and used in the previous analysis. The raw data used in this analysis were processed in the same way as in [1] and [2], including corrections for the energy loss of charged particles in the target, uncertainties in the magnetic field, and misalignments of drift chambers.

3 Analysis

3.1 Event Selection

In this analysis we are interested to identify the reaction $\gamma p \to pK^0\bar{K}^0$, however in reality in the final state we detect the proton, and K_S via it's decay to $\pi^+\pi^-$, so the reaction is $\gamma p \to pK_SX$. We require that the missing particle is another neutral kaon, which could be either K_S or K_L. For simplicity hereinafter we call the missing particle K_L. Thus, events for this analysis are selected requiring at least three charged tracks in the final state identified as a proton, π^+ and π^-. The initial photon is chosen to be within 1 ns of the start time defined by the start counter, and it was required to have only one hit in the tagger within 1.5 ns of the start time. The K_S is reconstructed in the invariant mass of two pions and K_L in the missing mass of detected particles, $M(K_L)^2 = M_X(pK_S)^2 = (P_\gamma + P_t - P_{K_S} - P_p)^2$, where P_i are four momenta of the photon, target proton, K_S and final state proton, respectively. The search for a resonance in

the KN system can be done either in the invariant mass of the proton and K_S or in the missing mass of K_S.

3.2 Reconstruction of Final State

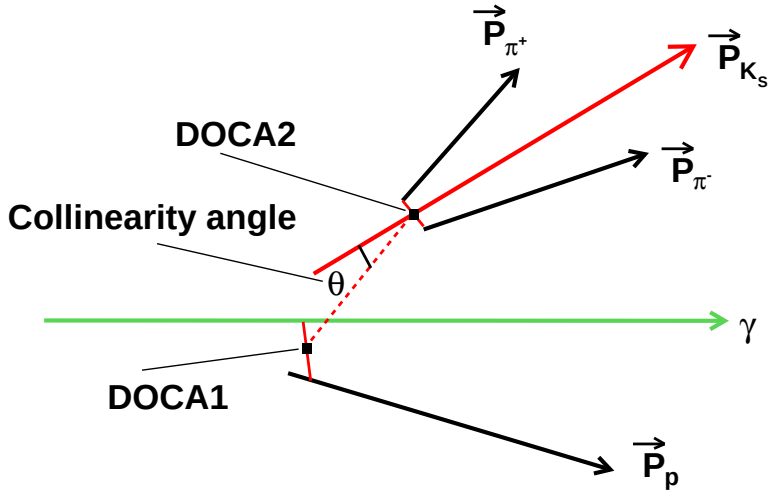

Figure 1: Reconstruction of final state

To identify the reconstructed K_S and the final KN state with a good mass resolution and acceptable signal to background ratio the following cuts were implemented (hereinafter referred to as vertex cuts, see Fig. 1):

1. The proton track must come with the closest distance not more than 1 cm from the photon beam line (this distance is called hereinafter DOCA1); the mid-point of the shortest line between the proton track and the photon beam line is called the primary vertex.

2. The distance of the mutual closest approach of the two pion tracks must be less than 0.5 cm (it is called hereinafter DOCA2); the mid-point of the shortest line between the two pion tracks is called the decay vertex.

3. $\cos\theta_c > 0.98$. The collinearity angle, θ_c, is the angle between the line connecting the primary and decay vertices and the direction of the three-momentum of the K_S reconstructed as the sum of the two pion momenta.

4. Decay distance $d > 3$cm. Decay distance is a distance between the primary and secondary vertex.

In the first CLAS publication in this channel [1] besides "no cut on vertices" approach, where no resonance was observed in pK system, the attempt was made to search for a narrow resonance using some of the vertex cuts defined above to suppress the background, however this didn't lead to the observation of any resonance structure either.

In particular the following cuts have been applied to data: a) DOCA2<1 cm, b) d> 3 cm, and DOCA1<2 cm. There were no collinearity angle restrictions have been applied to data. As a result the signal over background ratio S/B=5.2 and S/B=0.8 was obtained for the K_S and K_L peaks presented here in Fig. 2 from the CLAS Note preceding the publication [1]. Below In Fig. 3 we show the same plots with our vertex cuts described above. As one can see much cleaner peaks of both K_S and K_L are obtained with significant improvement of signal to background ratio. Numerically, the corresponding ratios for K_S and K_L are S/B=25 and S/B=2.2 respectively.

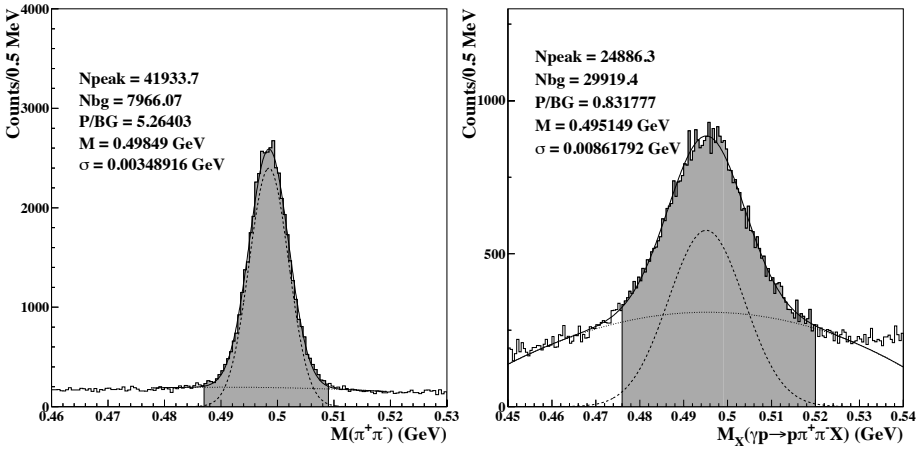

Figure 8.4: Left: $(\pi^+\pi^-)$ invariant mass distribution and the K_S peak. Right: missing mass distribution of the pK_S system and the missing kaon peak. The background under the K_S and missing kaon peaks is significantly reduced by applying the detached vertex cut.

Figure 2: Detailed figures from the CLAS Note. The corresponding figure in the published paper [1] is Fig.10..

In Fig. 4 we present missing mass of the proton for events with $M(\pi^+\pi^-) = 0.498 \pm 0.009$ GeV and $M_X(p\pi^+\pi^-) = 0.496 \pm 0.020$ GeV. The vertical bar at 1.035 GeV shows border line between the ϕ peak, about 3σ away from the ϕ peak, and the non-resonance $K\bar{K}$ production region. The ϕ peak fitted with Gaussian+Pol(2) (second order polynomial) function resulted in $M(\phi)$=1.022 GeV with Gaussian width σ=4.7 MeV.

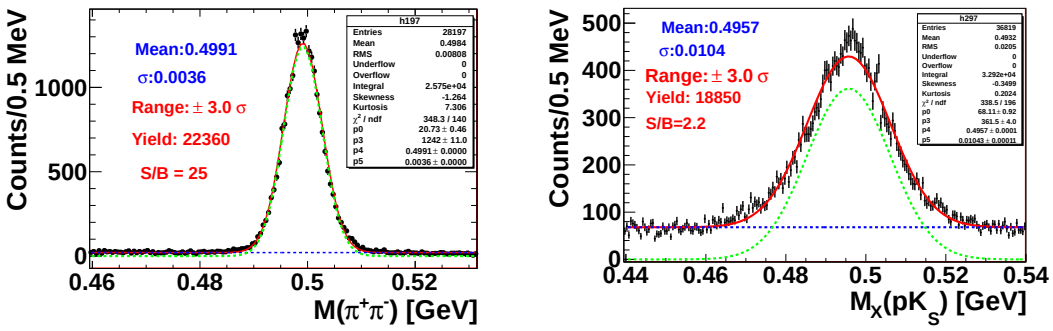

Figure 3: Left panel: Invariant mass of $\pi^+\pi^-$ pairs for events with $M_X(p) > 1.04$ GeV and $M_X(p\pi^+\pi^-) = 0.497 \pm 0.020$ GeV. Right panel: Missing mass of $M(p\pi^+\pi^-)$ with the same cuts, now with $M_X(p\pi^+\pi^-) = 0.499 \pm 0.01$ GeV.

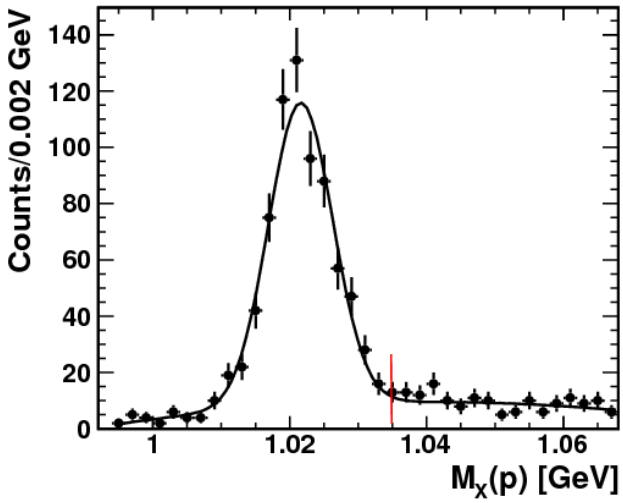

Figure 4: Missing mass $M_X(p)$ for events with $M(\pi^+\pi^-) = 0.498 \pm 0.004$ GeV and $M_X(p\pi^+\pi^-) = 0.497 \pm 0.020$ GeV.

4 Missing mass $M_X(K_S)$ in the reaction $^1H(\gamma, K_S)X$

Below the search for a baryon resonance in pK system is performed in a direct production for the range of the proton missing mass above the ϕ peak, $M_X(p)$ >1.035 GeV. In Fig. 5 we present Dalitz plot distribution for events above the ϕ peak, $M_X(p) > 1.035$ GeV. As one can see there is a huge bump in the higher masses of $pK_S(\pi^+\pi^-)$, therefore one has to search for a resonance structure in the missing mass $M_X(K_S(\pi^+\pi^-))$ to avoid reflections from the pK_S system. Therefore in the next Fig. 6 we present distribution of $M_X(K_S)$ with different cuts on the upper limit of $M(pK_S)$. As one can see the resonance structure appears at 1.55GeV and

becomes more and more prominent at lower upper limit cuts on $M(pK_S)$ avoiding reflections from excited Σ^*'s decaying to pK_S. In Fig. 7 we present $M_X(K_S)$ with the cut $M(pK_S) < 1.52$ GeV with all cuts apllyied in Fig. 6 and also a cut on a ground state $\Lambda(1116)$, $M(p\pi^-) > 1.126$ GeV. As one can see very prominent narrow resonance structure is observed at 1.550 ± 0.004 GeV. Statistical significance of the observed peak estimated is $S/\sqrt{(B)} = 9\sigma$. The contribution from the tail of the ϕ peak estimated from the Monte Carlo simulation appeared to have a small contribution (histogram with pink color).

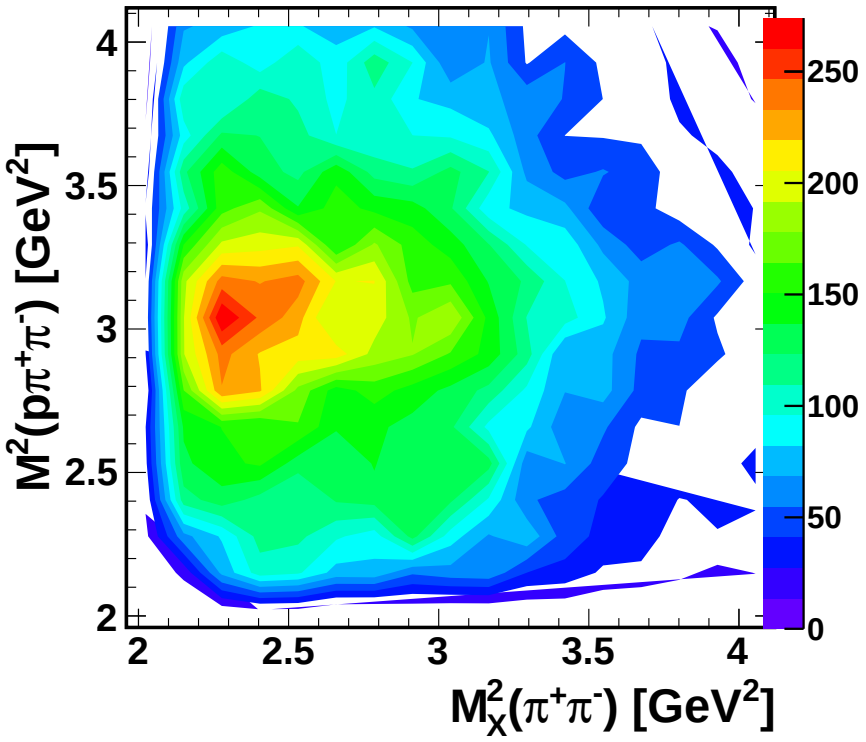

Figure 5: Dalitz plot $M^2(p\pi^+\pi^-)$ versus $M_X^2(\pi^+\pi^-)$.

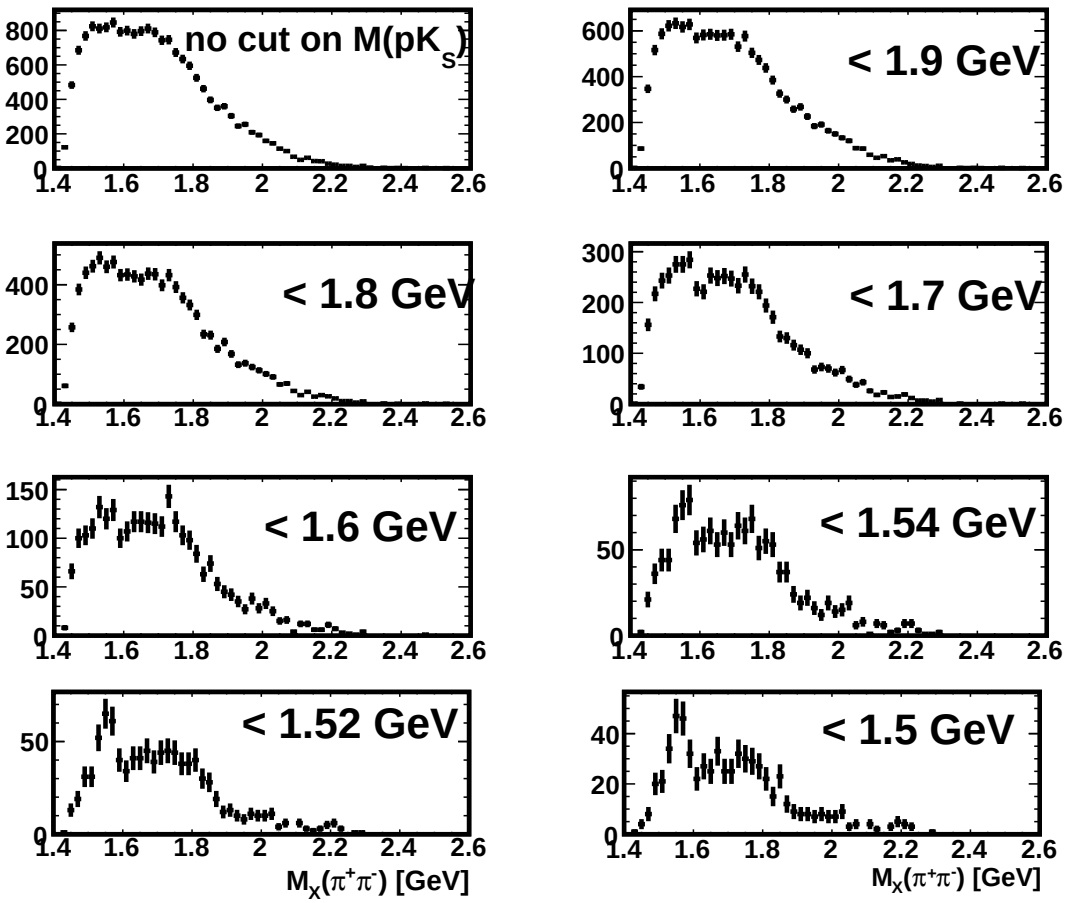

Figure 6: Missing mass $M_X(K_S)$ with different upper limit cuts on $M(pK_S)$.

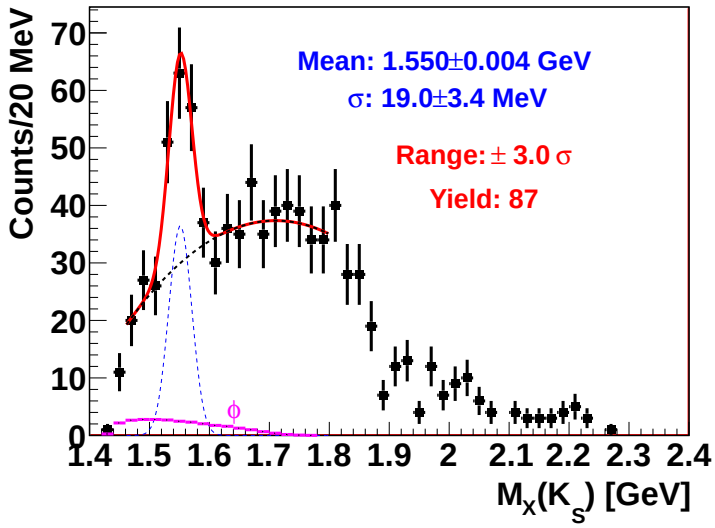

Figure 7: Missing mass $M_X(K_S)$ for events above the ϕ peak, $M_X(p) > 1.035$ GeV, with $M(pK_S) < 1.52$ GeV and $M(p\pi^-)$ >1.126 GeV. Fit is performed with Gaussian+POL(3) function. Lower histogram (with pink color) shows contribution of ϕ tail above $M_X(p) > 1.035$ GeV obtained with ϕ Monte Carlo used in [2].

5 Stability of the observed signal

To make sure that observed resonance structure is not due to the fine tuning of cuts we perform the following studies. Below we check the stability of the signal against the variation of all cuts used in Fig. 6 summarized in Table 1.

Table 1: Set of Cuts used in Fig. 6.

DOCA1 <	DOCA2 <	d >	$\cos\theta$	$\Delta M(\pi^+\pi^-)$	$M_X(p)$ >	$M(pK_S)$ <
1 cm	0.5 cm	3 cm	0.98	4 MeV	1.035 GeV	1.52 GeV

In Fig. 8 we present distribution of all vertex variables when all others are fixed to the values in Table 1 . In the next sections we will show how distribution of the missing mass $M_X(K_S)$ changes depending on the different cuts applied to the one selected variable.

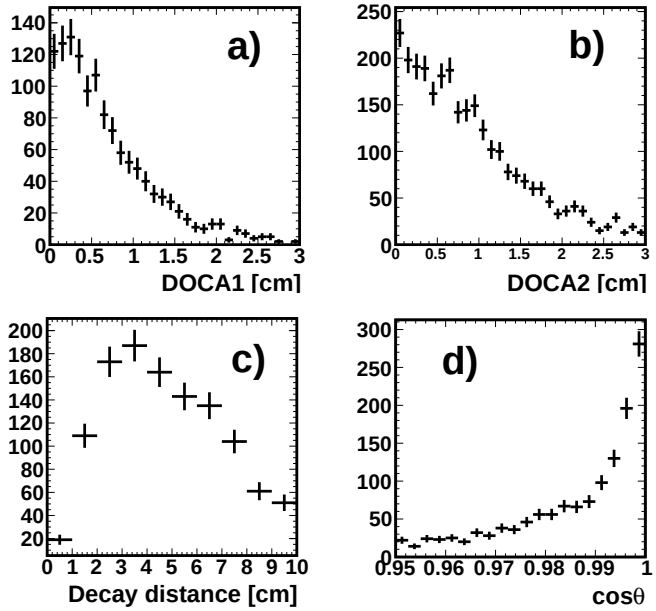

Figure 8: Distribution of different vertex cuts when all other cuts are fixed to the values in Table 1 except the one, which is plotted: a) DOCA1, b) DOCA2, c) Decay distance, d) Collinearity angle, $\cos\theta$.

5.1 Primary vertex

In Fig. 9 the stability of the resonance was checked against the DOCA1 cut by varying it in the range of 1.0-2.5 cm and leaving all other cuts unchanged. As one can see the sensitivity of observed peak to this cut is very weak.

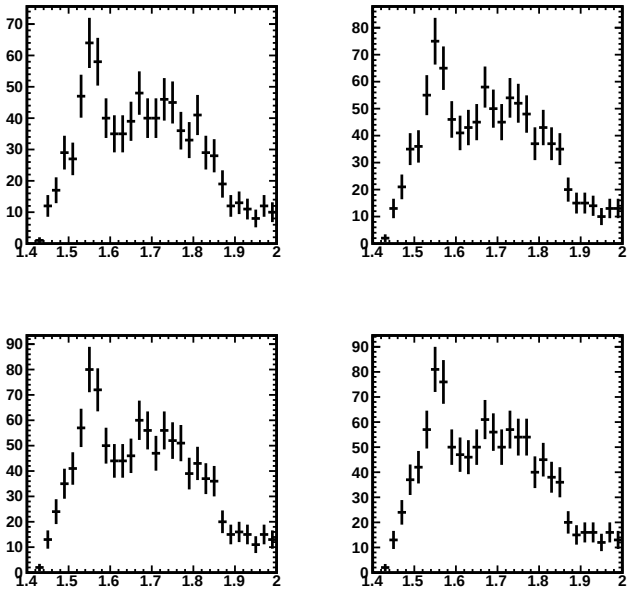

Figure 9: Missing mass $M_X(K_S)$ with different cuts on DOCA1: a) DOCA1< 1.0 cm, b) DOCA1< 1.5 cm, c) DOCA1< 2.0 cm, d) DOCA1< 2.5 cm

5.2 Decay vertex

In Fig. 10 the $M_X(K_S)$ is plotted with all other cuts fixed, but different cuts on DOCA2. The cut on DOCA2 is varied in the range 0.3-1.0 cm. The CLAS resolution to the distance of closest approach of two charged tracks is $\sim$0.3 cm [3], therefore the fact that signal remains prominent in the range 0.3-0.7 cm should be considered satisfactory.

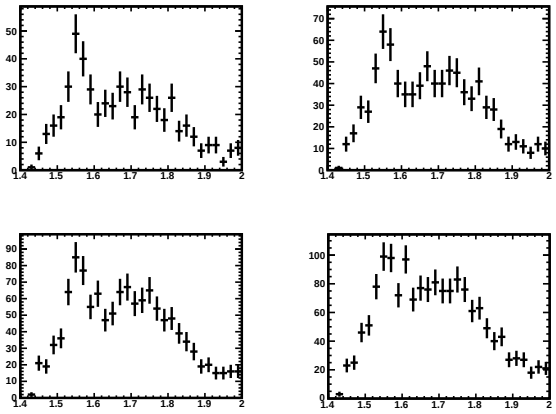

Figure 10: Missing mass $M_X(K_S)$ with different cuts on DOCA2: a) DOCA2<0.3 cm, b) DOCA2<0.5 cm, c) DOCA2<0.7 cm, d) DOCA2< 1.0 cm.

5.3 Decay distance

In Fig. 11 the $M_X(K_S)$ is plotted with fixed cuts on ..., but different cuts on decay distance d.

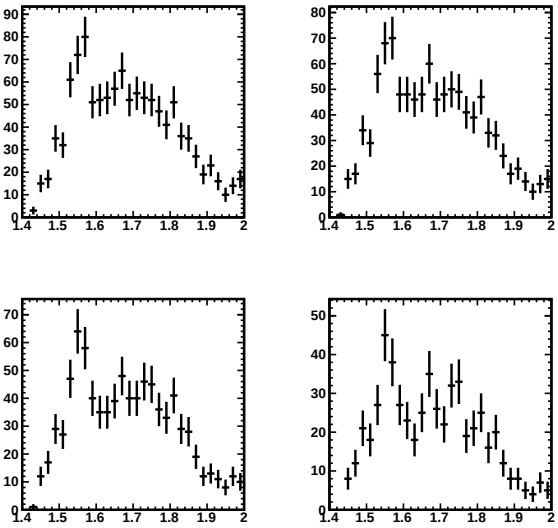

Figure 11: Missing mass $M_X(K_S)$ with different cuts on a decay distance: a) $d > 0$ cm, b) $d > 2$ cm, c) $d > 3$ cm, d) $d > 5.0$ cm.

5.4 The collinieality angle

In Fig. 12 the $M_X(K_S)$ is plotted with all other cuts fixed, but different cuts on $\cos\theta$.

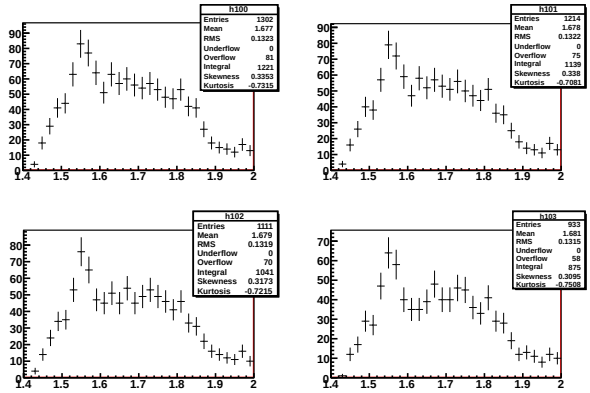

Figure 12: Missing mass $M_X(K_S)$ with different cuts on a decay distance: a) $\cos\theta > 0.95$, b) $\cos\theta > 0.96$, c)$\cos\theta > 0.97$, d) $\cos\theta > 0.98$.

5.5 Cut on $\Delta M(\pi^+\pi^-)$

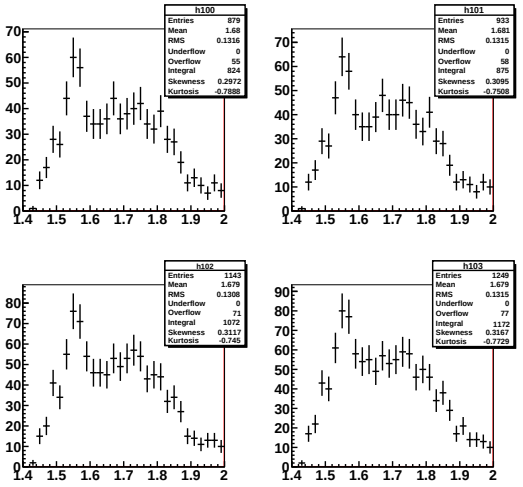

Figure 13: Missing mass $M_X(K_S)$ with different cuts on $\Delta M(\pi^+\pi^-)$: a) 3.6 MeV, b) 4.0 MeV, c) 6.0 MeV, d) 8.0 MeV.

5.6 Cut on $M_X(p)$

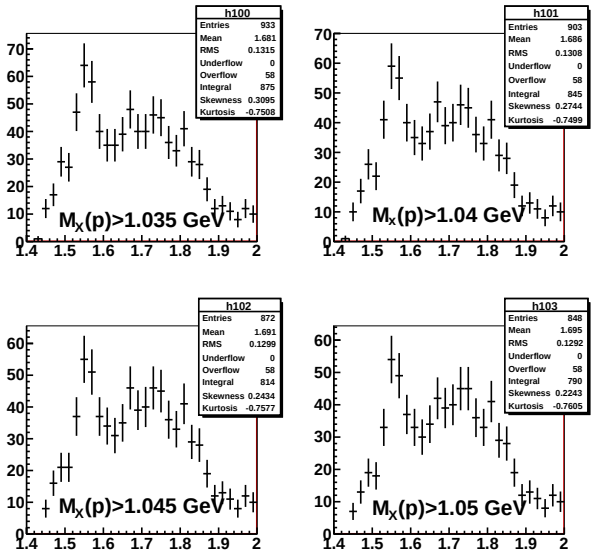

Figure 14: Missing mass $M_X(K_S)$ with different cuts on $M_X(p)$: a) $M_X(p) > 1.035$ GeV, b) $M_X(p) > 1.04$ GeV, c) $M_X(p) > 1.045$ GeV, d) $M_X(p) > 1.05$ GeV.

6 Data Sampling

Data sampling is a powerful method for hypotheses testing. The statistical power of the g11 data allows to divide them into two independent samples and see if the observed structure persists in both of them. First on Fig. 15 we show $M_X(K_S)$ for the whole statistics of g11 run with the following cuts: DOCA1<1 cm, DOCA2<0.75 cm, decay distance d> $3cm$, collinearity angle $\cos\Theta_c > 0.97$ and $M(pK_S)$ <1.52 GeV. To check the stability of the observed signal, we divided data into two chronologically separated distinct run periods with equal number of events. In Fig. 16 we present $M_X(K_S)$ for both parts. Statistical significance in the first part is estimated to be $R_1 = \frac{S}{\sqrt{B}} = 7.8\sigma$ while in the second part it is $R_2 = \frac{S}{\sqrt{B}} = 5.7\sigma$. Combined statistical significance of these two parts is $R = \sqrt{R_1^2 + R_2^2} = 9.5\sigma$, consistent with 10σ for the combined data.

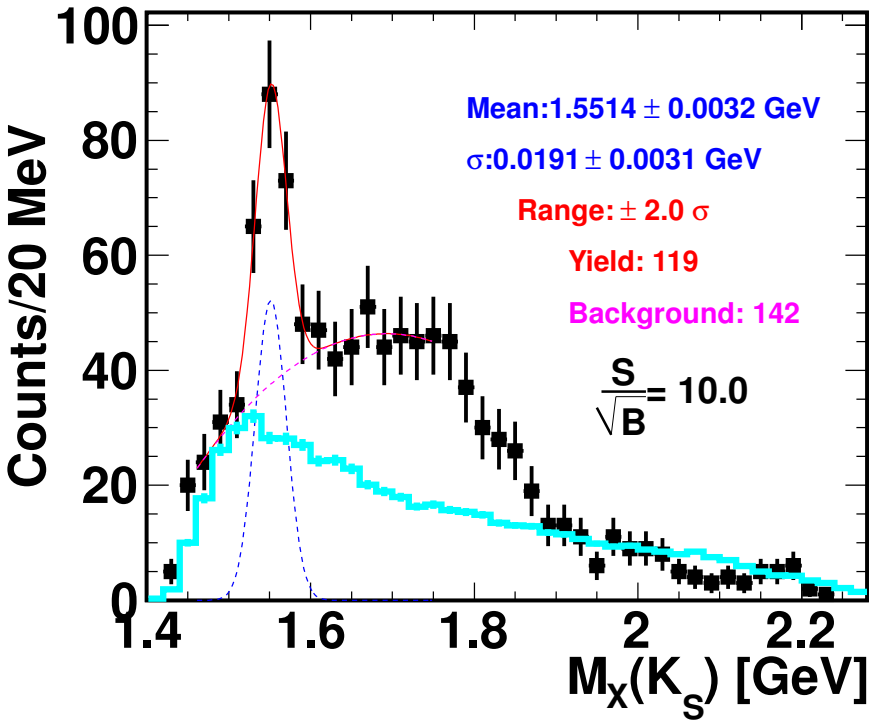

Figure 15: Missing mass, $M_X(K_S)$ with a cut $M(pK_S) < 1.52$ GeV for the whole g11 run. The solid (red) curve is a result of the fit with Gaussian+Pol(2) function. The dashed (blue) curve is Gaussian function from the fit and the background is presented by dotted (pink) curve. The solid histogram (cyan) is a result of phase space MC simulation.

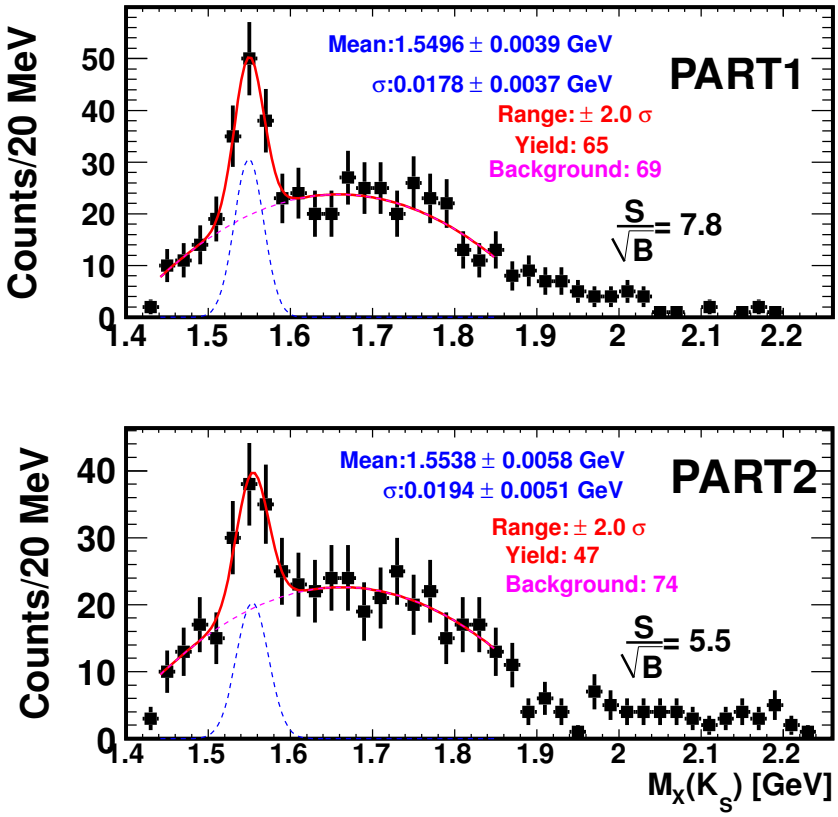

Figure 16: Missing mass, $M_X(K_S)$ with a cut $M(pK_S) < 1.52$ GeV. Upper plot is for the first part of g11a data, and lower panel is for the second part of g11a. Filled squares are data. Solid (red) curve is a result of the fit with Gaussian+Pol(2) function. In both panels dashed (blue) curve is Gaussian function from the fit and the background is presented by dotted (pink) curve.

7 The t_Θ-dependence

In our previous paper on interference [2] we hypothesized strong t_Θ dependence of the observed structure, where $t_\Theta = (P_\gamma - P_{K_S})^2$ is a four momentum transfer from the photon to K_S. Below in Fig. 7 we present missing mass, $M_X(K_S)$, distribution with different cuts on t_Θ.

Evidently, at stricter cuts the background under the peak drops faster than the signal itself, which means that the signal is more concentrated at small t_Θ, than the background. This confirms our previous conjecture about strong t_Θ dependence of the observed structure in Ref. [2].

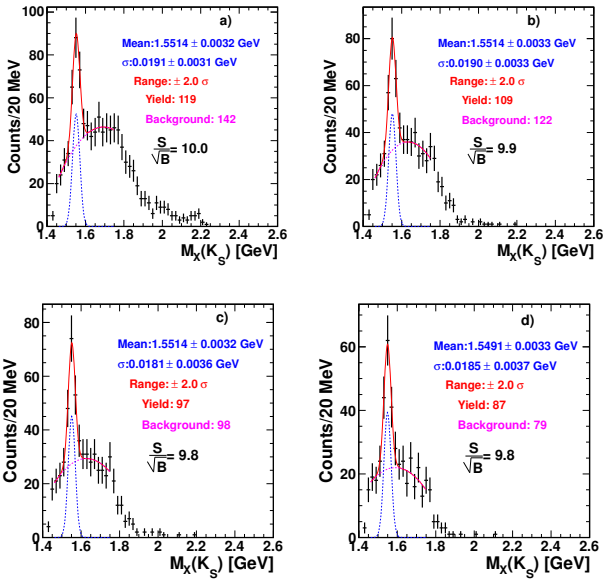

Figure 17: (Color online) Missing mass, $M_X(K_S)$ (counts per 20 MeV bin) for $M(pK_S) <$ 1.52 GeV with the following cuts: a) no cut on t_Θ, b) $|t_\Theta| < 0.85$ GeV^2, c) $|t_\Theta| < 0.75$ GeV^2, d) $|t_\Theta| < 0.65$ GeV^2. Solid (red) curve is a result of the fit with Gaussian+Pol(2) function.

The possibility to make the CLAS acceptance more favorable at lower t values is provided by selecting higher separation of primary and decay vertices, as larger decay distance correspond to higher momenta of K_S. In Fig. 7 we present the ratio of number of events with decay distance d >10cm over number of events with d >3cm with all other cuts unchanged. As one can see by selecting events with $d > 10cm$ higher values of t are less preferable, which should suppress higher masses in the missing mass $M_X(K_S)$ more than the peak at ~ 1.55 GeV as it has sharper t-dependence.

In Fig. 7 we present distribution of $M_X(K_S)$ with a cut on K_S decay distance d>10cm as compared to d>3cm used in the previous $M_X(K_S)$ distributions. As one can see the region of higher masses is suppressed much more than the peak itself. Although the statistical significance of the peak doesn't change, the fact that entire distribution outside of the peak drops significantly gives further confidence that the observed peak is real.

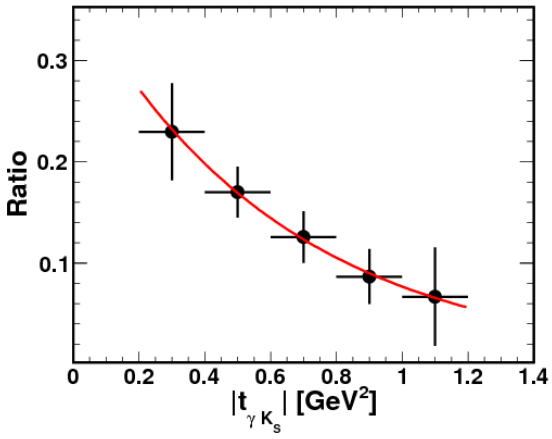

Figure 18: Ratio of number of events with decay distance d >10cm over number of events with d >3cm versus four-momentum transfer $-t_{\gamma K_S}$.

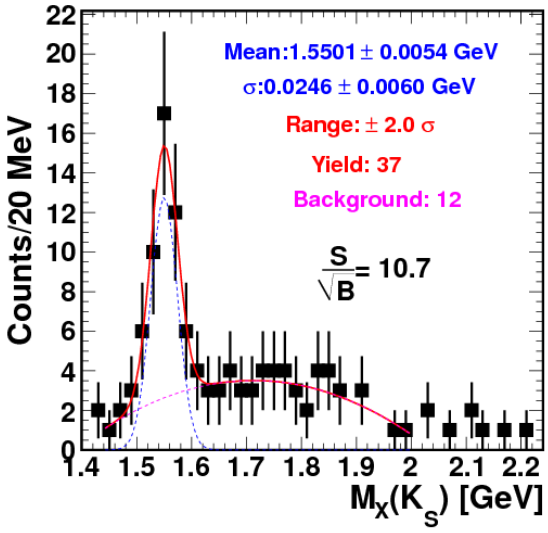

Figure 19: Missing mass, $M_X(K_S)$ with a cut $M(pK_S) < 1.52$ GeV, but with decay distance d>10cm. Filled squares are data points. Solid (red) curve is a result of the fit with Gaussian+Pol(2) function. Dashed (blue) curve is Gaussian function obtained from the fit and the background is presented by dotted (pink) curve.

8 The $M(pK_S)$ invariant mass

Observation of the baryon resonance in the missing mass of K_S rises the question about manifestation of the same resonance in the invariant mass of the proton and K_S, $M(pK_S$. Although theoretically there is no difference between detected and missing kaons, as both of them are not flavor eigenstates and are admixtures of K^0 and $\bar{K}^0$, nevertheless in the real experiment these two channels have very different acceptances in CLAS and different mass resolutions and in principle are not symmetric. Below we describe our search for baryon resonance in the invariant mass $M(pK_S)$. In fig. 20 we present distribution of $M_X(K_S) = M(pK_L)$ and $M(pK_s)$ before and after the acceptance corrections with the same following cuts: $\cos\theta > 0.95$, DOCA1<1 cm, DOCA2<0.7 cm, $M_X(p) > 1.035$ GeV, $M(pK_S)(pK_L) < 1.5$ GeV. a) missing mass $M_X(K_S)$ before acceptance correction, b) same as a) for $M(pK_S)$, c) missing mass $M_X(K_S)$ after acceptance correction d) both $M(pK_L)$ (red circles) and $M(pK_S)$ (black squares), the blue histogram is phase-space Monte Carlo simulated histogram. As one can see after the acceptance correction, seemingly not so evident signal in the invariant mass $M(pK_S)$ becomes more prominent and, which is striking, almost coincides with the $M(pK_L)$ distribution without additional normalization.

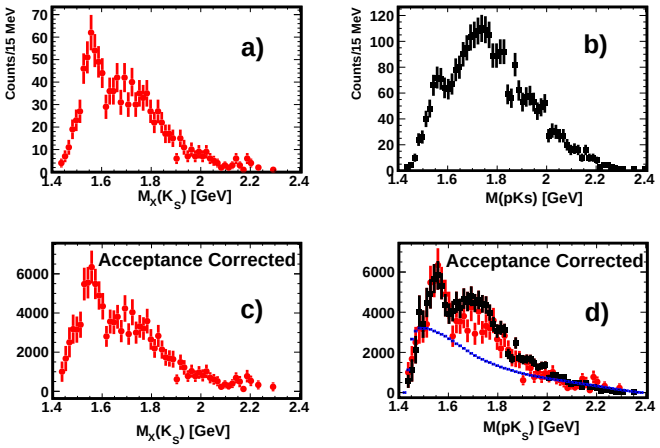

Figure 20: Distribution of $M_X(K_S) = M(pK_L)$ and $M(pK_s)$ before and after the acceptance corrections with the same following cuts: $\cos\theta > 0.95$, DOCA1<1 cm, DOCA2<0.7 cm, $M_X(p) > 1.035$ GeV, $M(pK_S)(pK_L) < 1.5$ GeV. a) missing mass $M_X(K_S)$ before acceptance correction, b) same for $M(pK_S)$, c) missing mass $M_X(K_S)$ after acceptance correction d) both $M(pK_L)$ (red circles) and $M(pK_S)$ (black squares), the blue histogram is phase-space Monte Carlo simulated histogram.

9 Summary

In this note we presented new results on the search for narrow strange baryon resonance in the reaction $\gamma p \to pK_SK_L$. The resonance structure is observed in both missing mass $M_X(K_S)$ and invariant mass $M(pK_S)$ at ~ 1.550 GeV and narrow Gaussian width 19 ± 3 MeV compatible with experimental resolution. Statistical significance of the observed peak estimated as $R = S/\sqrt{(B)}$

is as high as 10σ. Formally, the strangeness of the observed structure is not defined, as both K_S and the the missing kaon are not flavor eigenstates. However the absence of similar structure outside of missing kaon peak, which corresponds to the decay of unknown state to $\Lambda\pi^+(\Sigma^\pm\pi^\mp)$, lead us to conclude that it is unlikely for the observed structure to be due to yet unobserved excited Σ^{*+} state, alternatively it could be due to an exotic state consistent with Θ^+ pentaquark. To tag the strangeness would require to perform a search in K^+n system.

References

[1] R. De Vita *et al.* [CLAS Collaboration], Phys. Rev. D **74**, 032001 (2006) [arXiv:hep-ex/0606062].

[2] M. Amaryan *et al.*, Phys. Rev. **C85**, 035209, (2012) .

[3] B. Mecking *et al.*, Nucl. Inst. and Meth. A **503**, 513 (2003).

[4] M. Battaglieri and R. De Vita, CLAS ANALYSIS NOTE 2006-103.